Power Electronics Thermal Management R&D

Annual Report

Gilbert Moreno

NREL is a national laboratory of the U.S. Department of Energy
Office of Energy Efficiency & Renewable Energy
Operated by the Alliance for Sustainable Energy, LLC

This report is available at no cost from the National Renewable Energy Laboratory (NREL) at www.nrel.gov/publications.

Management Report
NREL/MP-5400-64943
April 2016

Contract No. DE-AC36-08GO28308

NREL
NATIONAL RENEWABLE ENERGY LABORATORY

Power Electronics Thermal Management R&D

Annual Report

Gilbert Moreno

Prepared under Task No. VTP2.7301

NREL is a national laboratory of the U.S. Department of Energy
Office of Energy Efficiency & Renewable Energy
Operated by the Alliance for Sustainable Energy, LLC

This report is available at no cost from the National Renewable Energy Laboratory (NREL) at www.nrel.gov/publications.

National Renewable Energy Laboratory
15013 Denver West Parkway
Golden, CO 80401
303-275-3000 • www.nrel.gov

Management Report
NREL/MP-5400-64943
April 2016

Contract No. DE-AC36-08GO28308

Cover Photos by Dennis Schroeder: (left to right) NREL 26173, NREL 18302, NREL 19758, NREL 29642, NREL 19795.

NREL prints on paper that contains recycled content.

I. Power Electronics Thermal Management R&D

Principal Investigator: Gilbert Moreno
National Renewable Energy Laboratory (NREL)
Transportation and Hydrogen Systems Center
15013 Denver West Parkway
Golden, CO 80401
Phone: 303-275-4450
E-mail: gilbert.moreno@nrel.gov

DOE Technology Development Manager: Susan A. Rogers
U.S. Department of Energy
1000 Independence Ave. SW EE-3V
Washington, DC 20585
Phone: 202-586-8997
E-mail: susan.rogers@ee.doe.gov

NREL Task Leader: Sreekant Narumanchi
Phone: 303-275-4062
Email: sreekant.narumanchi@nrel.gov

Abstract

The objective for this project is to develop thermal management strategies to enable efficient and high-temperature wide-bandgap (WBG)-based power electronic systems (e.g., emerging inverter and DC-DC converter). Device- and system-level thermal analyses are conducted to determine the thermal limitations of current automotive power modules under elevated device temperature conditions. Additionally, novel cooling concepts and material selection will be evaluated to enable high-temperature silicon and WBG devices in power electronics components. WBG devices (silicon carbide [SiC], gallium nitride [GaN]) promise to increase efficiency, but will be driven as hard as possible. This creates challenges for thermal management and reliability.

Accomplishments

- We conducted steady-state and transient analyses to compare the thermal performance of the 2012 Nissan LEAF power module to the performance of a more conventional power module design (power module that incorporates a metalized-ceramic substrate).
- We evaluated the effect of increasing the junction temperatures (up to 250°C) on an automotive power module (2012 Nissan LEAF) to simulate WBG conditions. Results indicated the need for high-temperature attach materials (e.g., sintered silver) for WBG-based power modules.
- We determined that a direct-cooled direct-bond copper (DBC) configuration is superior to a direct-cooled baseplate configuration when the convective thermal resistance values are lower than 20 mm^2-K/W.
- We used a particle image velocimetry (PIV) system to measure flow fields of an impinging liquid jet in an attempt to understand heat transfer enhancement mechanisms and improve power electronics thermal management. The high-heat transfer rates of jet impingement cooling provide a way to achieve convective resistance values lower than 20 mm^2-K/W.

✧ ✧ ✧ ✧ ✧

Introduction

This project will analyze and develop thermal management strategies for WBG-based power electronics systems. Research will be conducted to evaluate thermal management strategies at the device and system levels. Device-level research will focus on die and substrate-integrated cooling strategies and heat transfer enhancement technologies. System-level research will focus on thermal management strategies for the entire power electronics system to enable smart packaging solutions. One challenge with WBG device power electronics is that although losses in the form of heat are lower, the area of the devices is also reduced to increase power density and reduce costs associated with the use of WBG materials. This creates higher heat fluxes that must be removed from a smaller footprint, and combined with higher operational temperatures requires advanced thermal management strategies.

Several strategies may be implemented to improve thermal management:

- Concepts related to die/substrate-integrated thermal management
- Flow enhancements and enhanced surfaces
- Advanced manufacturing techniques
- Multiple mode cooling concepts
- Power electronics system-level thermal analysis for effective packaging.

Most of the current and past research efforts have been focused on power module-level cooling strategies. In this project, a system-level approach will be used to evaluate the thermal interactions between the various system components (i.e., power modules, capacitor, control boards) and their ambient under-hood environment. The trend towards high-temperature WBG devices emphasizes the need for system-level thermal management analysis. Although WBG devices can operate at higher temperatures (>200°C), other components (e.g., capacitors, attach layers, interconnects) may not tolerate the higher temperatures, and thus system-level analysis and innovative cooling strategies are required to allow for reliable system operation.

Approach

Work conducted in this project can be grouped into two categories—application thermal research, and thermal and fluid measurement systems. Research conducted in the application thermal research category aims to understand the effects of high-temperature WBG-based devices on the power electronics components and develop thermal management strategies to enable WBG-based inverters. There are currently no automotive power electronics systems that use WBG devices. Therefore, an automotive silicon-based power electronics system will be modeled and used as the framework for the WBG analyses. The analyses will begin at the power module level and then expanded to include all of the inverter components.

Research conducted in the thermal and fluid measurements systems works to develop thermal measurement techniques to understand heat transfer mechanisms and to develop novel packaging materials. The following provides more details on the project approach.

Application thermal research

- Create and validate thermal computational fluid dynamics (CFD) and finite element analysis (FEA) models of an automotive power electronics system.
- Use the models to evaluate the effects of incorporating high-temperature WBG devices on other system components (e.g., power module attach layers, capacitors, electrical boards, interconnects). Identify thermal bottlenecks within the system and map out system temperatures.
- Generate thermal management concepts to enable the use of WBG-based inverters.

Thermal and fluid measurement systems

- Measure fluid flow fields using PIV to understand heat transfer and improve heat exchanger designs.
- Quantify the performance of novel high thermal performance materials using the phase-sensitive transient thermoreflectance (PSTTR) system.

Results and Discussion

A model of the 2012 Nissan LEAF inverter was used for the thermal analyses. Images of the LEAF power electronics systems are shown in Figure 1. The system consists of three power modules that are mounted onto a cast-aluminum cold plate and associated electronic components (e.g., capacitors, electrical boards, and interconnects). The cold plate is integrated into the inverter housing and cools the power modules by circulating water-ethylene glycol (WEG) through a series of channels. Figure 2 shows a computer-aided design (CAD) rendering of a LEAF power module. The power modules consist of three insulated gate bipolar transistor (IGBT)-diode pairs per switch position. The cross-sectional view shown in Figure 2 provides a detailed view of the power module layers and interfaces.

In the Electric Drive Technologies (EDT) Thermal Performance Benchmarking project, computational fluid dynamics and FEA models of the 2012 LEAF power modules and cooling system were created and validated using experimentally obtained data. Those models were modified and used for the analysis work in this project.

The LEAF modules do not use metalized-ceramic substrates (e.g., direct -bond-copper or DBC substrates) for electrical isolation. Instead, the LEAF modules incorporate a thin, rubber-like dielectric pad mounted between the power modules and the cold plate for electrical isolation (Figure 1). A grease thermal interface material (TIM) is applied on both sides of the dielectric pad to reduce thermal contact resistance.

Figure I-1: Pictures of the 2012 Nissan Leaf inverter. The middle image shows the cold plate cooling channels. Image on the right shows one power module mounted on the cold plate. The dielectric pad and TIM layers are shown (right).
Photo Credits: Gilbert Moreno (NREL)

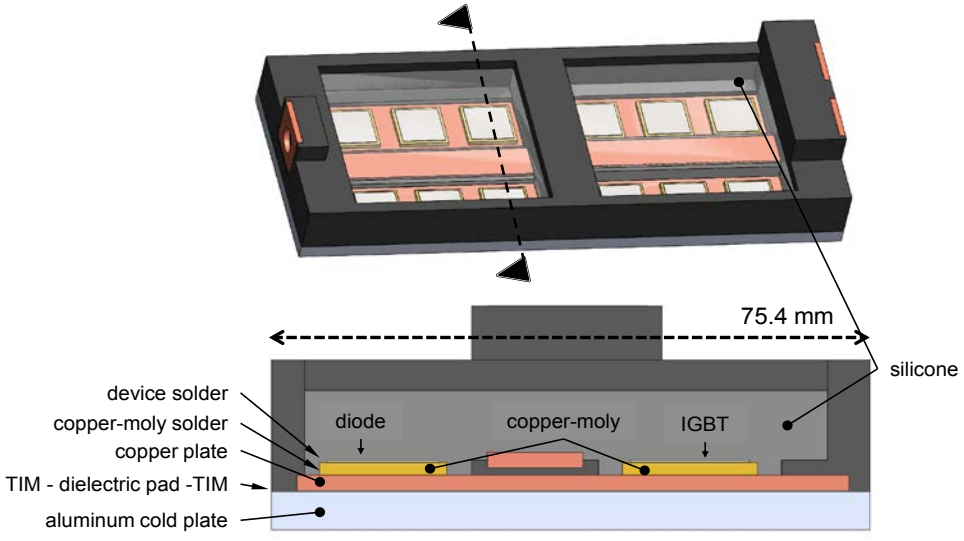

Figure I-2: CAD model of the Nissan Leaf power module. The top image shows the entire module. The various power module layers are shown in the lower, cross-sectional view. The interface bonding layers are labeled on the lower image.

LEAF Power Module Thermal Analyses

An analysis was conducted to compare the thermal performance of the LEAF power module design with the performance of a more conventional metalized-ceramic substrate module design. For these analyses, the LEAF power module model was modified to eliminate the copper-moly sheets and dielectric pad and incorporate a DBC substrate (Figure 3). The DBC substrate consisted of a 0.38-mm-thick alumina sheet with two 0.25-mm-thick copper layers on both sides. Steady-state FEA simulations were then carried out using both the LEAF design (standard) and the LEAF DBC configuration design at various convective thermal resistance values. Figure 4 shows an FEA-generated temperature contour plot for a maximum junction temperature of 200°C. Figure 5 provides the total thermal resistance versus the convective thermal resistance for the standard LEAF module, the LEAF module with the DBC configuration, and a Semikron SKM module. The total specific thermal resistance was defined per Equation 1.

$$R''_{th,j-f} = \frac{T_{j,max} - T_f}{Q_{IGBT}} \times A_{IGBT} \qquad \text{Equation 1}$$

where $T_{j,max}$ max is the maximum junction, T_f is the fluid temperature, Q_{IGBT} is the heat dissipated per insulated-gate bipolar transistor (IGBT), and A_{IGBT} is the area of the IGBT (225 mm^2).

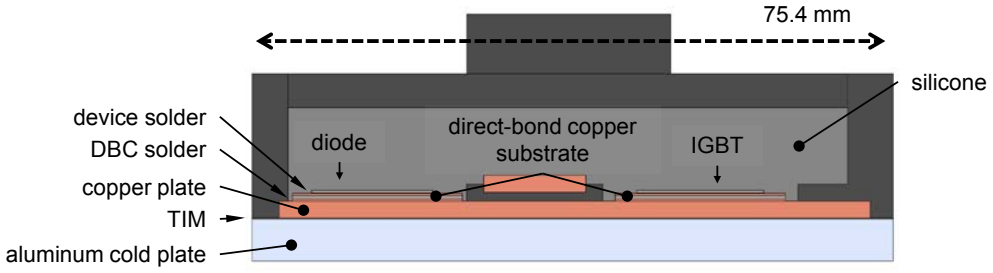

Figure I-3: Cross-sectional view of the LEAF module configuration that incorporates a DBC substrate.

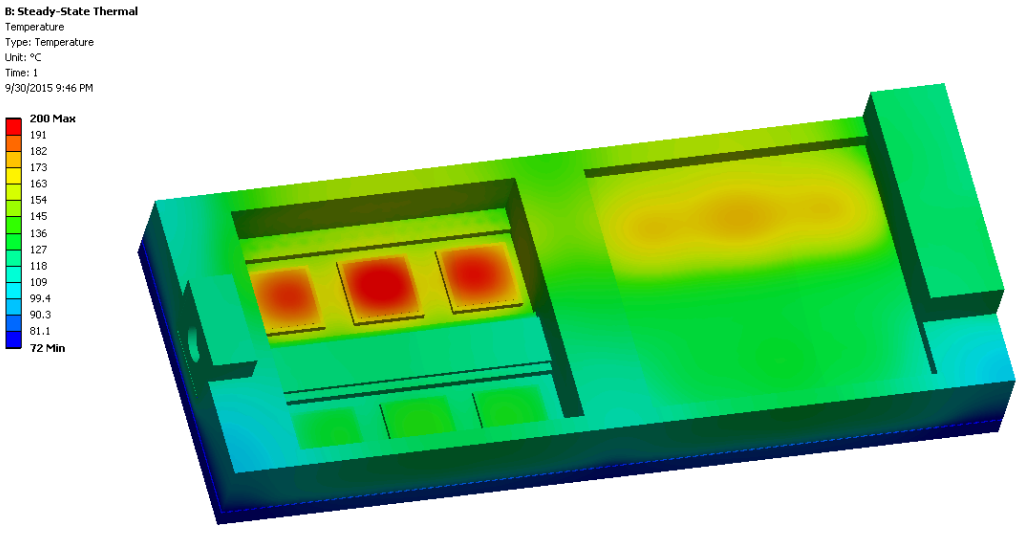

Figure I-4: FEA-generated temperature contours for the LEAF module. The left side has the silicone encapsulant hidden to reveal the devices.

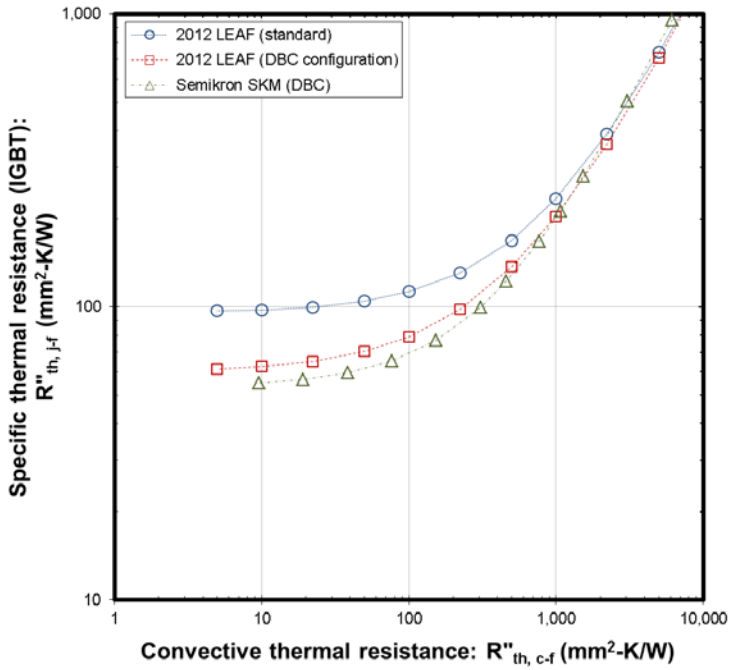

Figure I-5: Specific (junction-to-liquid) thermal resistance plotted versus the convective thermal resistance for three different power module configurations. The Semikron SKM data were taken from Bennion and Moreno [1].

Only one power module was modeled, and a three-to-one (IGBT-to-diode) heat loss ratio was used in the simulations. The total power dissipated through the modules was adjusted so that the maximum junction temperatures reached 200°C at every convective thermal resistance condition. The convective thermal resistance was imposed as a heat transfer coefficient boundary condition on the aluminum cold plate lower surface. A 70°C temperature was used for the fluid temperature. The LEAF module material properties values used are provided in Thermal Performance Benchmarking Project FY15 year-end report.

As shown in Figure 5, the total thermal resistance for the LEAF (standard) power module is greater than the total thermal resistance for the DBC configuration module—approximately 30% greater at R"th, c-f = 100 mm^2-K/W. The performance of the DBC configuration LEAF module is similar to the performance of the Semikron SKM module that also incorporates a DBC substrate, which helps to confirm the performance of a typical DBC-based power module. Moreover, power modules using highly thermally conductive ceramic substrates (e.g., aluminum nitride DBC) will have a lower thermal resistance as compared with the power modules shown in Figure 5.

FEA simulations were also conducted to compare the transient thermal performance of the LEAF (standard) power module with the performance of the DBC configuration power module. Figure 6 plots the thermal resistance of two module designs (LEAF standard and DBC-LEAF variant) for the case when the power modules are initially at a uniform temperature of 70°C and power to the devices was turned on (i.e., increasing temperature condition). The total heat imposed in the power modules was 2,084 W and 2,956 W for the LEAF and DBC-LEAF variant, respectively. A three-to-one (IGBT-to-diode) heat loss ratio and a convective thermal resistance of 100 mm^2-K/W with a fluid temperature of 70°C were used for transient simulations. In Figure 6, the thermal impedance was defined per Equation 2.

$$Z_{th,\,j-f}\,(t) = \frac{T_{j,max}\,(t) - T_f}{Q_{IGBT}} \qquad \text{Equation 2}$$

where $T_{j,max}(t)$ is the maximum junction temperature as a function of time.

The transient thermal impedance for the LEAF (standard) module was found to be lower (~40% lower at 60 milliseconds) than the thermal impedance for the DBC configuration LEAF module at time scales below one second. At time scales greater than one second, the thermal impedance of the LEAF (standard) module become

greater than the thermal impedance of the DBC-LEAF as conditions approach steady-state operation. These results suggest that there may be some transient benefits to the LEAF module design. Moreover, the LEAF module may also offer cost and reliability advantages over the conventional metalized-ceramic substrate modules.

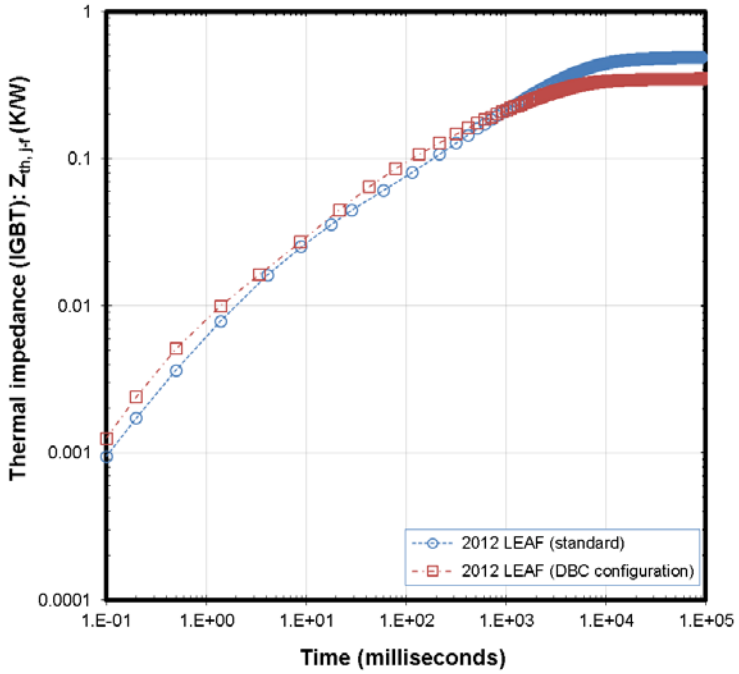

Figure I-6: Junction-to-liquid thermal impedance plotted versus time for two different power module configurations.

Effect of Increased Junction Temperatures on Module Attach Layers

FEA steady-state simulations were conducted to evaluate the effect of increasing the device temperatures on the power module solder and TIM layers. The elevated temperature conditions were intended to simulate the high temperatures associated with WBG devices. The 2012 LEAF power modules model was used for this study (Figure 2). The FEA simulations were conducted using the same process used to generate results provided in Figure 4 (vary the total heat dissipated by the devices to obtain a desired maximum junction temperature). The convective-cooling heat transfer boundary condition was applied to the lower aluminum cold plate surface. A 70°C temperature was used for the fluid temperature. SiC properties were used for the devices to simulate WBG power modules. The properties for all other components were the same material properties used to generate Figures 4- 6.

Maximum solder and TIM temperatures were computed at five maximum junction temperatures. The results are provided in Figure 7. A junction temperature of 125°C is intended to simulate temperature conditions for silicon devices, and junction temperatures greater than 150°C are intended to mimic WBG temperature conditions. Figure 7 shows three plots corresponding to three convective thermal resistance conditions. The higher convective thermal resistance of 100 mm^2-K/W and 50 mm^2-K/W are more representative of conventional WEG and channel flow cooling systems. The lower convective thermal resistance value of 10 mm^2-K/W represents a more effective cooling strategy (e.g., two-phase cooling).

At a junction temperature of 250°C, the solder layers at both the die and copper-moly attach interfaces exceed 220°C (melting temperature for Sn-Ag-Cu solders [2]) for all three convective thermal resistance conditions. Increasing the convective cooling performance was found to have minimal effect on the two solder interface layers. For example, the copper-moly solder maximum temperature only decreases by approximately 3°C when going from a convective cooling resistance of 100 mm^2-K/W to a convective cooling resistance of 10 mm^2-K/W (for the 250°C junction temperature case). Results clearly indicate that high-temperature bonding materials (e.g., sintered silver) are required for high-device temperature operation. The results provided in

Figure 7 may be a useful resource for power module manufacturers that are designing WBG-based power electronic systems.

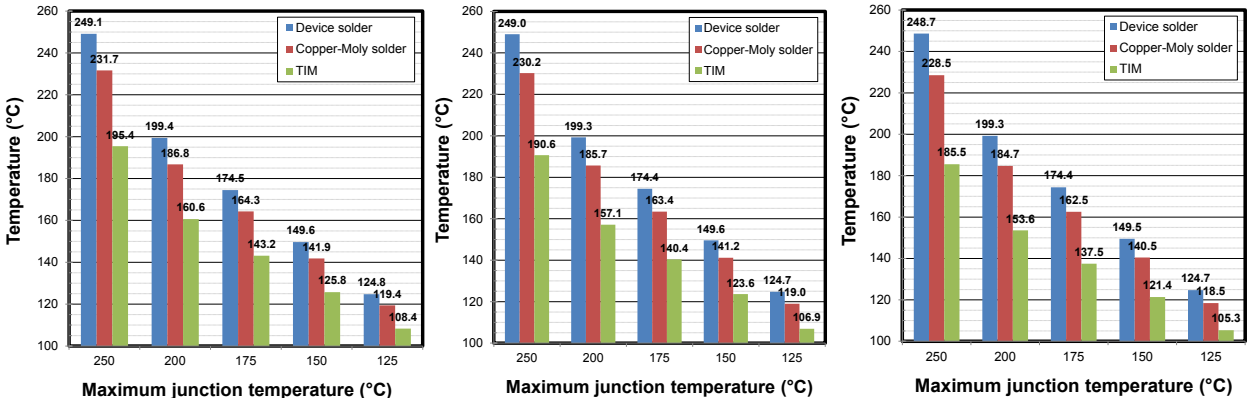

Figure I-7: The maximum temperatures for the device solder, copper-moly solder, and TIM layers at five different junction temperatures. Temperatures are provided for three different convective cooling thermal resistance values– 100 mm^2-K/W (left), 50 mm^2-K/W (middle), and 10 mm^2-K/W (right).

Work in FY15 was limited to power module thermal analyses. In FY16, we will expand our analyses to incorporate the entire LEAF inverter.

Evaluation of Direct-Cooled DBC and Direct-Cooled Baseplate Configurations

An objective of this project is to evaluate and develop new thermal management strategies that are applicable to traditional and WBG-based power electronic systems. Therefore, a parametric study was conducted to evaluate direct-cooled DBC and direct-cooled baseplate configurations (Figure 8). The direct-cooled DBC configuration provides cooling directly on the back side of the DBC substrate. The direct-cooled baseplate configuration provides cooling on the back side of the baseplate. The concept is to minimize the thermal resistance of the passive stack layers to reduce the total thermal resistance. However, the strategy of removing packaging layers limits the module's heat spreading ability; therefore, this strategy is best utilized when combined with low convective thermal resistance configurations. In this section, we evaluate various module designs to determine under what convective cooling conditions it makes sense to employ a direct-cooled DBC configuration.

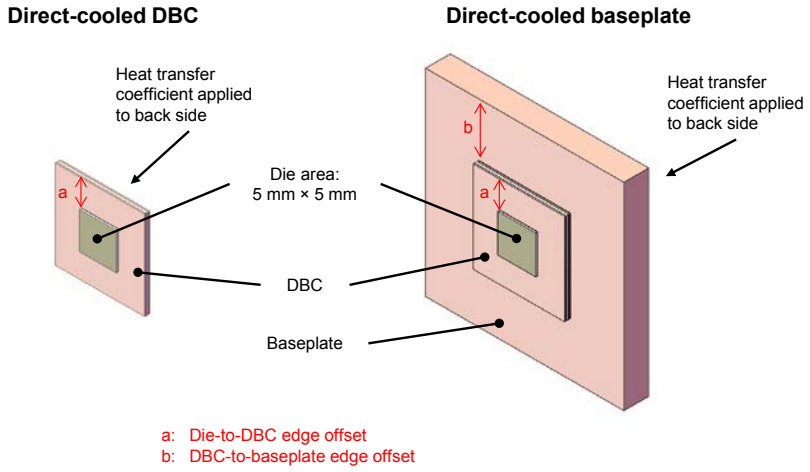

Figure I-8: CAD renderings showing the geometry of the direct-cooled DBC (left) and direct-cooled baseplate (right) configurations. FEA was conducted to evaluate the effect of varying the a and b dimensions on the total thermal resistance.

Steady-state FEA simulations were conducted to evaluate the effect of varying the DBC and baseplate dimensions on the total thermal resistance. Figure 8 shows the two CAD models used for the FEA. The power

modules shown in Figure 8 are representative of a typical power module design (e.g., they are not commercially-available modules). The materials used for this analysis are shown in Table 1.

Table I-1: Materials used for the module show in Figure 8

	Layer	
Direct cooled DBC	SiC (device)	Direct cooled Baseplate
	Solder	
	Cu	
	SiN (substrate)	
	Cu	
	Solder	
	AlSiC (baseplate)	

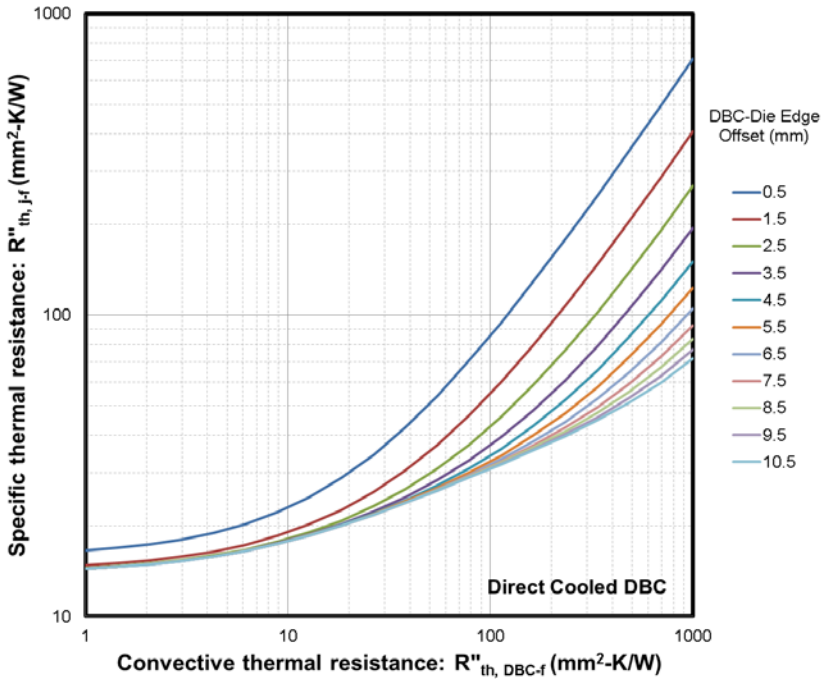

Figure I-9: Specific thermal resistance plotted versus the convective thermal resistance for different DBC-to-die edge offset values.

Figure 9 plots the total thermal resistance versus the convective thermal resistance for the direct-cooled DBC configuration. Various curves corresponding to different DBC-to-die distances (a) are shown in the figure. As shown, the effect of increasing the DBC size (dimension "a" in Figure 8) depends on the convective cooling

performance. The heat spreading effects of a larger DBC size are more beneficial at higher convective thermal resistance values (e.g., air cooling).

Figure 10 plots the total thermal resistance versus the convective thermal resistance for two direct-cooled baseplate configurations. In Figure 10, the effect of varying the baseplate-to-DBC distance ("b" dimension in Figure 8) on the total thermal resistance is evaluated. Two die-to-DBC offset values were considered: 3.5 mm (left plot in Figure 10) and 7.5 mm (right plot in Figure 10). Similar to the direct-cooled DBC configuration, the effect of changing the baseplate-to-DBC size ("b" dimension in Figure 8) depends on the convective thermal resistance. The benefits of increasing the baseplate-to-DBC size on the total thermal resistance are minimal at lower convective thermal resistance values. At higher convective resistances varying the baseplate-to-DBC offset value has more of an impact on the total thermal resistance for the case with the smaller (3.5 mm) die-to-DBC distance.

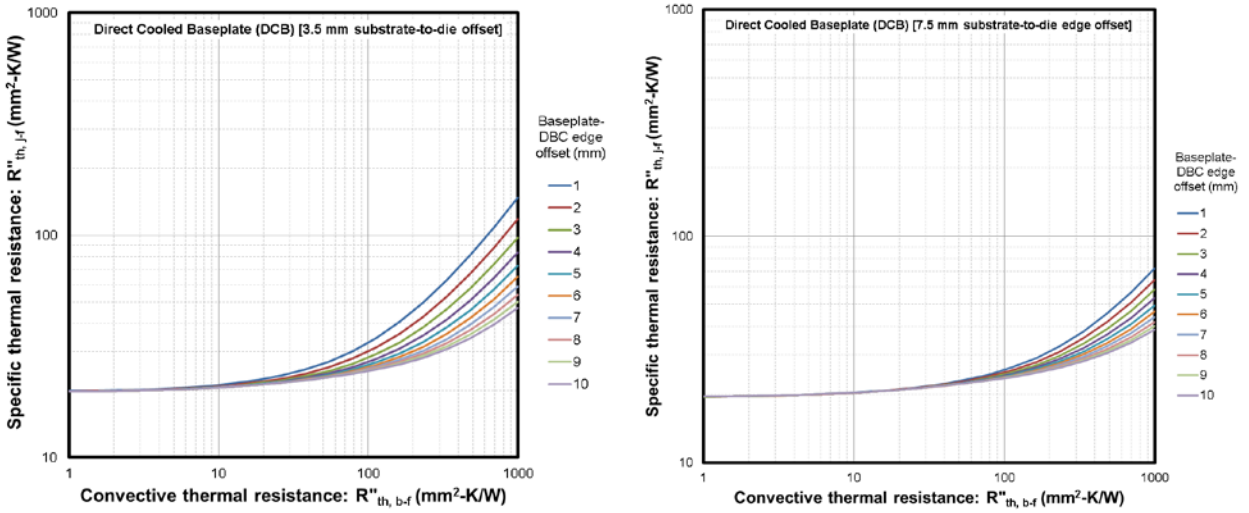

Figure I-10: Specific thermal resistance plotted versus the convective thermal resistance for different baseplate-to-DBC edge offset values. The plot on the left uses a 3.5 mm die-to-DBC distance, and the plot on the right uses a 7.5 mm die-to-DBC distance.

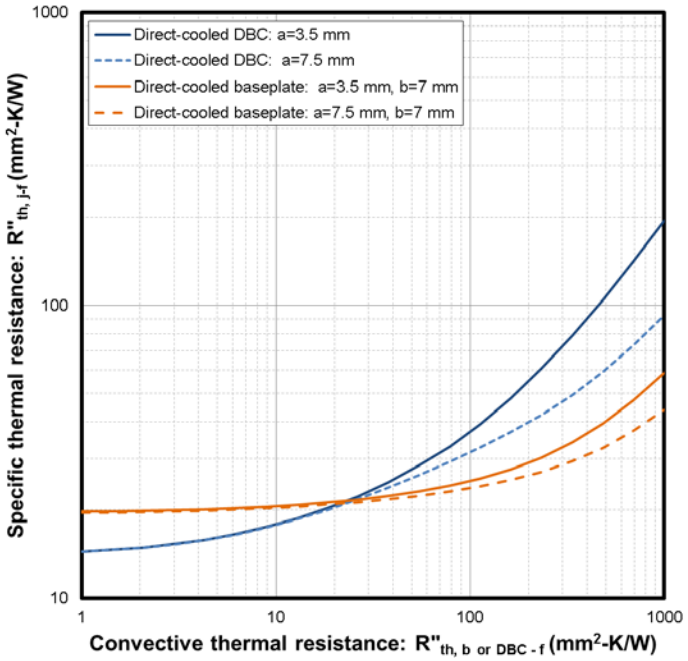

Figure I-11: Specific thermal resistance plotted versus the convective thermal resistance for DBC- and baseplate-cooled configurations.

Figure 11 plots the direct-cooled DBC and direct-cooled baseplate curves on the same graph. The figure indicates that direct cooling the DBC is superior to direct cooling the baseplate at convective thermal resistance values less than 20 mm^2-K/W. Achieving a convective thermal resistance value less than 20 mm^2-K/W (equivalent to an overall heat transfer coefficient value greater than 50,000 W/m^2-K) would likely require the use of micro-channels and/or impinging jets in a single-phase liquid cooling configuration or the use of two-phase heat transfer. In this analysis the layer dimensions were not constrained based on package space limitations. Applications constrained by space or requiring the dies to be packaged closely would benefit more from low convective thermal resistance cooling techniques as compared to applications where devices are spaced farther apart.

Measurement of Jet Impingement Flow Fields using PIV

Prior work at NREL has demonstrated that enhanced surfaces (e.g., roughened, microporous, micro-finned) can significantly increase jet impingement heat transfer [3]. In that study, the heat transfer increases were measured, but the mechanisms responsible for the enhancements were not fully understood. In this project, we used a PIV system to measure fluid flow fields and thus understand the underlying mechanisms responsible for the jet impingement heat transfer improvements associated with enhanced surfaces.

Figure 12 shows a picture and schematics of the PIV system. The PIV system was used to measure the flow fields of an impinging liquid (water) jet. Initial tests were conducted using a submerged-jet configuration. Future tests will be conducted using a free-jet configuration. The PIV system consists of a laser, camera, computer, and associated electronics. To visualize the fluid flow, the fluid must first be seeded with micrometer-sized particles that follow the motion of the fluid. A laser is used to illuminate the particles, allowing the camera to track the particles' motion. A 100-cm-long pipe with a 6-mm-inner diameter metal tube was used as the nozzle for these tests. The length of the tube combined with average water flow rate (~2 m/s) created a fully developed turbulent jet at the tube/nozzle exit. The nozzle-to-target surface distance was maintained at 6 mm for all tests.

Figure 13 shows PIV-generated velocity contour plots for a submerged-jet impinging on a roughened surface. The velocity magnitude, fluctuating component of the radial velocity, and the fluctuating component of the axial velocity were computed by averaging 1,000 data sets. The fluctuating velocity components (i.e., RMS velocity) are used to quantify the amount of turbulence within a flow. PIV data have been collected for smooth

and roughened surfaces. Work is currently underway to evaluate the data to determine the effect of the surface roughness on the flow within the wall-jet region. It has been hypothesized that the surface roughness features advance the laminar-to-turbulent flow transition within the wall-jet region and that this is the reason for the heat transfer enhancements. This study aims to experimentally evaluate this theory using PIV.

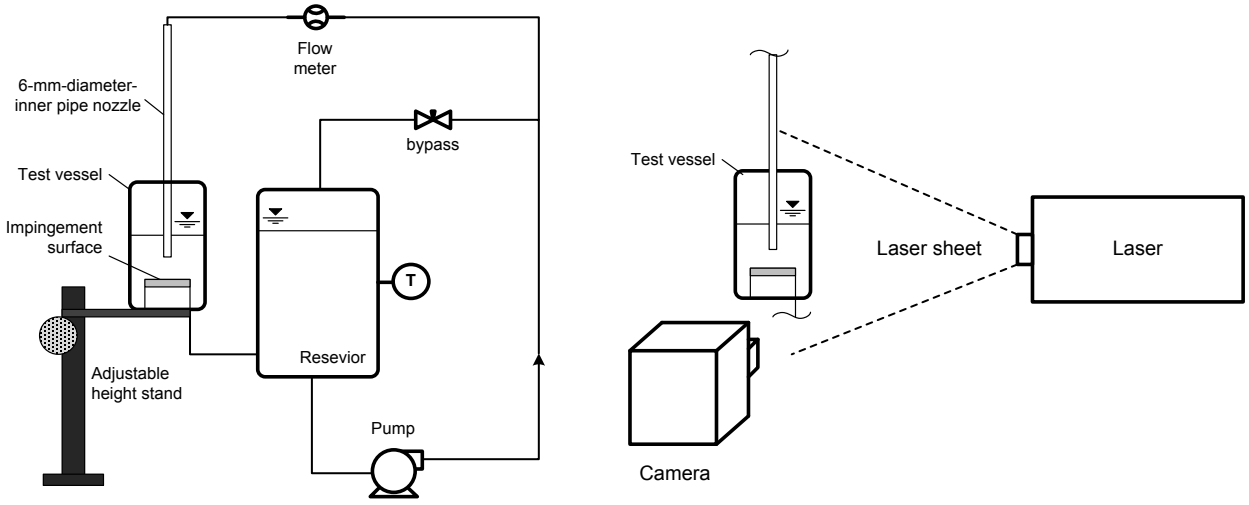

Figure I-12: PIV system schematics showing the piping layout (left) and the laser and camera setup (right).

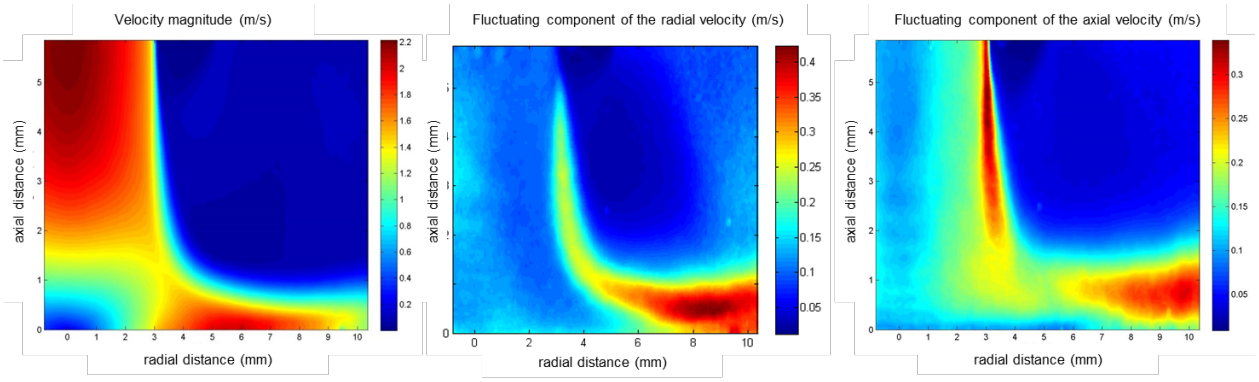

Figure I-13: PIV-generated velocity contour plots for a submerged jet impinging on a roughened surface. The velocity magnitude (left), fluctuating component of the radial velocity (middle), and the fluctuating component of the axial velocity (right) are shown.

Conclusions and Future Directions

Conclusions

- FEA simulations were conducted to compare the thermal performance of the 2012 Nissan LEAF power module to the performance of a more conventional power module design (power module that incorporates a metalized-ceramic substrate). Results indicate that the LEAF power module has a higher steady-state total thermal resistance (approximately 30% greater at R"th, c-f = 100 mm^2-K/W) as compared with a conventional power module design. However, the transient analysis indicates that the LEAF power module may offer advantages under certain transient conditions.
- The effect of elevating the device temperatures on the power module attach layers was evaluated. FEA simulations were conducted using maximum junction temperatures of 125°C, 150°C, 175°C, 200°C,

and 250°C. The higher junction temperatures were intended to simulate WBG devices. Temperatures for the component attach (e.g., solder and TIM) layers were computed. Results clearly indicate that high-temperature bonding materials (e.g., sintered silver) are required for high-temperature device operation.

- Direct-cooled DBC configurations were evaluated and compared with direct-cooled baseplate configurations. Analyses showed that direct-cooled DBC configurations are superior to direct-cooled baseplate configurations when the convective thermal resistance values are less than 20 mm^2-K/W. To achieve convective thermal resistance values less than 20 mm^2-K/W would likely require micro-channel, jet impingement, or two-phase heat transfer cooling strategies.
- PIV was used to measure flow fields for impinging liquid jets. Results from this work will help to understand how enhanced surfaces increase jet impingement heat transfer. This information can then be used to develop more effective power electronic heat exchangers.

Future Work

- System-level thermal analysis will be conducted to evaluate the effect of increased device temperatures on the inverter components (e.g., capacitors, interconnects, electrical boards). System hot spots and thermal bottlenecks will be identified. Thermal management solutions to enable WBG-based inverters will be proposed.
- PIV research efforts to understand heat transfer enhancement mechanisms in submerged- and free-jets will continue into FY16.
- NREL's PSTTR system will be used to quantify the performance of novel, high thermal performance materials.

Nomenclature

A	area
DBC	direct-bond copper
k	thermal conductivity
Q	heat
Rth	thermal resistance
R"th	specific thermal resistance
T	temperature
Z	impedance

Subscripts

b	baseplate
c	cold plate
f	fluid
j	junction

FY 2015 Presentations /Publications/Patents

1. Waye, S. “Power Electronics Thermal Management R&D.” Advanced Power Electronics and Electric Motors FY15 Kickoff Meeting, DOE Vehicle Technologies Office (VTO), Oak Ridge, TN, November 2014.
2. Bennion, K. “Power Electronics Thermal Management R&D.” 2015 DOE VTO Annual Merit Review, Crystal City, VA, June 2015.
3. Bennion, K. “Power Electronics Thermal Management R&D.” 2015 presentation to the DOE VTO Electrical and Electronics Technical Team, Southfield, MI, May 2015.

Acknowledgments

The author would like to acknowledge the support provided by Susan Rogers and Steven Boyd, Technology Development Managers for the EDT Program, Vehicle Technologies Office, U.S. Department of Energy Office of Energy Efficiency and Renewable Energy. The significant contributions of Kevin Bennion, Emily Cousineau, Charles King, and Xuhui Feng are acknowledged.

References

1. Bennion, K.; Moreno, G. 2010. “Thermal Management of Power Semiconductor Packages — Matching Cooling Technologies with Packaging Technologies.” Presented at 2nd Advanced Technology Workshop on Automotive Microelectronics and Packaging, Dearborn, MI. 26 pp. NREL/PR-540-48147.
2. Kester, 2010 "Alloy Temperature Chart" downloaded from www.kester.com/kester-content/.../Alloy-Temperature-Chart-15Feb11.pdf
3. Moreno, G.; Narumanchi, S.; Venson, T.; Bennion, K. 2013. "Microstructured Surfaces for Single-Phase Jet Impingement Heat Transfer Enhancements." ASME Journal of Thermal Sciences and Engineering Applications, 5(3), 031004, 9 pp. Paper No. TSEA-12-1033; doi: 10.1115/1.4023308.